

Optical probing of high-intensity laser interactions with underdense plasmas using the VULCAN petawatt laser facility

P.M. Nilson¹, S.P.D. Mangles¹, L. Willingale¹, M.C. Kaluza¹, A.G.R. Thomas¹,
Z. Najmudin¹, R.G. Evans¹, A.E. Dangor¹, K. Krushelnick¹, M. Tatarakis²,
R.J. Clarke³, K.L. Lancaster³, C. Hernandez-Gomez³, S. Karsch⁴
and J. Schreiber⁴

¹ *Department of Physics, The Blackett Laboratory, Imperial College, London SW7 2BZ, UK*

² *Technological Educational Institute of Crete, Chania, Crete, Greece*

³ *Central Laser Facility, CCLRC Rutherford Appleton Laboratory, Oxon OX11 0QX, UK*

⁴ *MPI für Quantenoptik, Garching, Germany*

1. INTRODUCTION

Ongoing developments in high-intensity laser technology have enabled continued progress in the study of relativistic laser-matter interactions. Of particular interest are the generation of relativistic electrons [1] and fast ions [2].

Despite the low absorption characteristics of gases, the VULCAN Petawatt Laser Facility, RAL, UK, offers a novel capability for studying energy absorption, heat transport and hydrodynamic expansion in underdense plasmas by delivering 100's J in a sub-ps laser pulse ($>10^{20} \text{ Wcm}^{-2}$), achieving an extreme-relativistic intensity regime. In this report, we present optical probing measurements of the initial stages of cylindrically symmetric blast wave formation in helium gas driven by the VULCAN Petawatt Laser.

Previously, the dynamics of strong blast waves have been studied extensively in various geometries [3], principally due to their role in the formation and evolution of astrophysical phenomena [4]. Laboratory studies of laser-driven blast waves have accessed both the early and late stages of blast wave formation by careful choice of target composition, laser energy, pulse duration, and focused intensity. Two important properties are observed; firstly, the front is observed to reduce in thickness over time and, secondly, the front exhibits instability after 200 ps following the termination of the laser pulse.

2. EXPERIMENT

The experiment was performed using the VULCAN Petawatt Laser at the Rutherford Appleton Laboratory. A schematic of the experimental layout is given in figure 1.

The laser delivered pulses of 200 J in 650 fs at a wavelength of $1.054 \mu\text{m}$ (Nd:glass). The laser was focused onto the edge of a supersonic gas jet target (2 mm nozzle diameter) using an $f/3$ off-axis parabolic mirror to a vacuum focal spot of $6\text{--}7 \mu\text{m}$ full width at half maximum, with a peak irradiance of $3 - 5 \times 10^{20} \text{ Wcm}^{-2}$. Helium was used as the target gas. The backing pressure could be varied to give plasma electron densities of up to $5 \times 10^{19} \text{ cm}^{-3}$. Analysis of the wavelength-shifted laser light scattered by the Raman forward scattering instability provided a simultaneous measurement of the plasma electron density during the interaction.

The interaction was diagnosed with a temporally independent probe beam in a direction orthogonal to the main interaction. The probe beam was derived from the compressed main beam, providing high temporal resolution, and frequency doubled to $0.527 \mu\text{m}$ in a KDP (potassium dihydrogen phosphate) crystal. The plasma evolution and blast front structure was monitored by re-imaging the probe beam with 10x magnification and approximately $5 \mu\text{m}$ resolution.

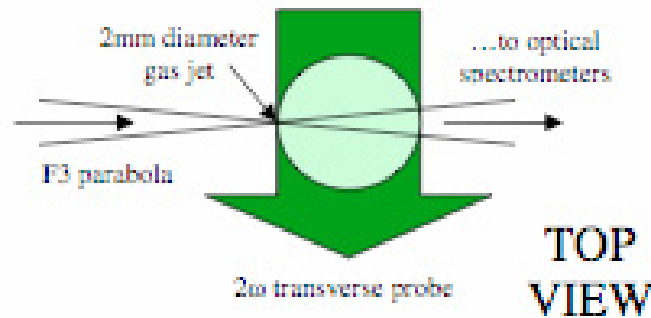


Figure 1. The experimental layout.

3. RESULTS

The plasma evolution was tracked in time to $t_0 + 225$ ps. We define t_0 to be the time that the main pulse arrives at the focal plane, marked B in figure 2 a). The inherent prepulse ensures that the main pulse will interact with a low-temperature, low density plasma.

Figure 2 displays shadowgrams taken at $t_0 + 10$ ps and $t_0 + 225$ ps. The laser has created a cylindrical channel over $350 \mu\text{m}$ in length prior to defocusing. At this stage, a cylindrically symmetric, smooth, radially propagating front has formed. The front is $70 \mu\text{m}$ in radius and $400 \mu\text{m}$ in length, expanding with a radial velocity of $7 \times 10^8 \text{ cm s}^{-1}$.

The laser is observed to filament as it defocuses into a cone of 9° half-angle. The filaments extend to the rear of the gas jet. The darkest regions of the filamentary structures indicate high-electron-density gradients where the probe beam has been refracted out of the acceptance angle of the optical system. Ionization tracks are evident at large angles to the rear of the gas jet. These are due to large-angle side-scattering instabilities.

Figure 2 (lower image) is a shadowgram taken at $t_0 + 225$ ps. The blast front has been driven into the ambient plasma. Instability has developed on the expanding front. Importantly, figure 3 demonstrates how this instability has developed without the front fragmenting or breaking-up. Rather, the front maintains

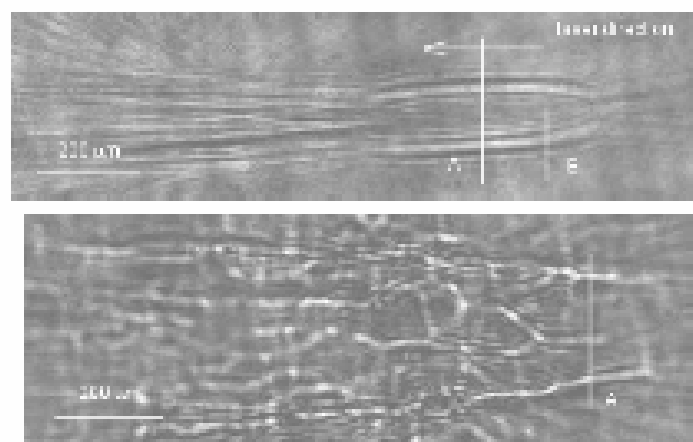


Figure 2. Shadowgrams taken at $t_0 + 10$ ps (above) and $t_0 + 225$ ps (below).

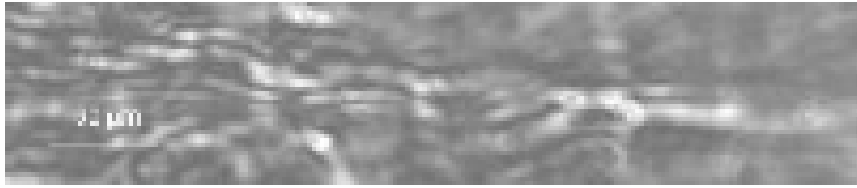


Figure 3. A shadowgram taken at t_0+225 ps highlighting the shock front instability.

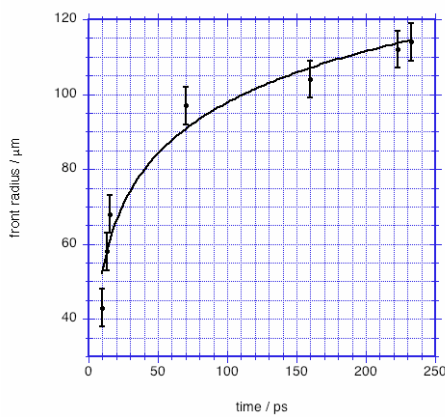


Figure 4. A plot of the temporal variation in blast front radius.

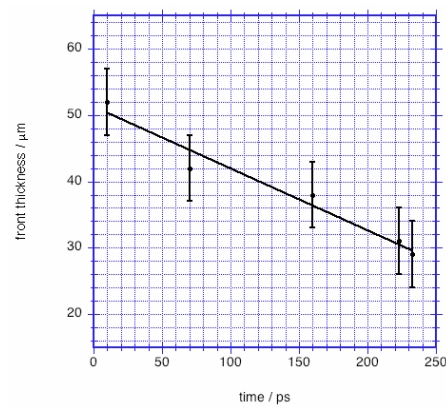


Figure 5. A plot of the temporal variation in blast front thickness.

an approximately uniform thickness, while the instability has a wavelength and amplitude on the scale of the front thickness itself.

Over a series of shots, the front trajectory was tracked in time by varying the delay of the probe beam with respect to the interaction beam. Figures 4 and 5 show how the blast front radius and thickness vary in time, respectively, along the radial position marked A. The blast front is observed to reduce in thickness from approximately $52 \mu\text{m}$ to $30 \mu\text{m}$ between $t_0 + 10$ ps and $t_0 + 225$ ps.

Following an initial stage of rapid expansion, the front velocity reduces from $7 \times 10^8 \text{ cm s}^{-1}$ to $1 \times 10^7 \text{ cm s}^{-1}$. The data in figure 4 are fitted to the expression $R = \beta t^\alpha$, where R is the blast front radius. The initial stage of expansion gives $\alpha = 1.06$ with maximum standard deviation 0.03. During the late stage of expansion, $\alpha = 0.18$ with maximum standard deviation 0.03.

4. PIC SIMULATIONS

We have undertaken a series of 2D3V particle-in-cell simulations using the code OSIRIS to study the first few picoseconds of plasma evolution. For the simulations presented below, a stationary box was used to observe the plasma evolution following the passage of a laser pulse with $a_0 = 15$.

The density profile of the fully ionized He plasma was modeled with a 0.1mm ramp to a density of $0.01n_{\text{cr}}$, maintained over 0.5mm. The linearly polarized laser beam had a Gaussian profile of 0.65 ps duration. The beam was focused to the top of the density ramp, corresponding to a power of 0.4PW. The computational grid has longitudinal (x) and transverse (y) dimensions of $587 \mu\text{m}$ and $168 \mu\text{m}$ respectively.

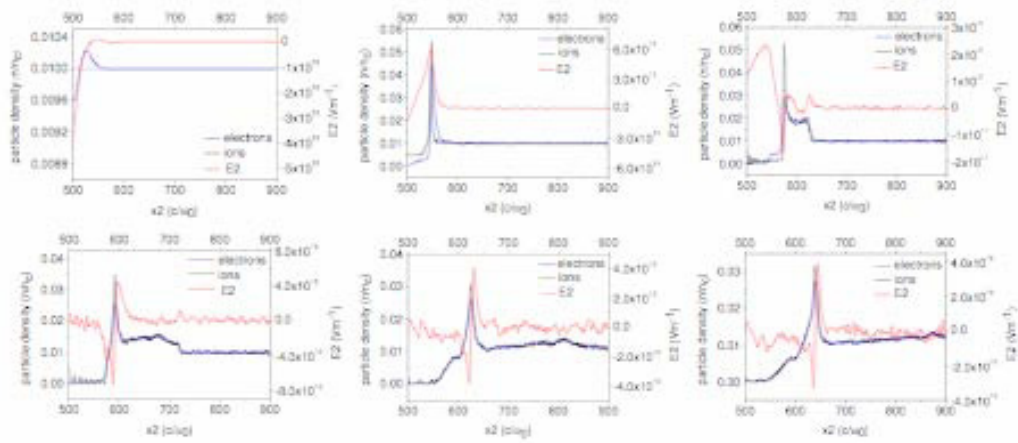


Figure 6. OSIRIS code results for different time steps (0.48 ps, 0.80 ps, 1.20 ps, 1.60 ps, 2.00 ps, 2.80 ps) showing the evolution of electron density, ion density, and the magnitude of the radial electric field. Note the scales vary on each graph.

Figure 6 shows the evolution of plasma parameters along a cross-section taken at the centre of the computational grid. Presented are profiles of n_e , n_i and E_2 (the electric field component in the transverse x_2 direction) as a function of x_2 . Only one side of the expanding plasma is given, where $x_2 = 500$ corresponds to the centre of the laser-generated plasma channel. Note that the scale varies on each plot.

After 0.48 ps, the electrons have responded to the laser ponderomotive force. They have been expelled from the axial region, setting up an electric field. The ions initially remain stationary by virtue of their greater inertia.

By 0.8 ps, the ions have had imparted upon them a significant impulse and have accelerated to the position of the electron front.

An electric field exists across the combined electron and ion front, caused by the more mobile electrons propagating slightly ahead of the ion front. By 1.2 ps, the electron-ion front is propagating at $\approx 10^8 \text{ cm s}^{-1}$ into the upstream ambient gas. We see evidence for a multi-group ion flux; the ions with greater momentum begin to propagate ahead of the main front, presenting a steep density gradient to the ambient gas. A sufficient population of electrons is tied to the forward propagating front, thereby maintaining quasi-neutrality. The lower energy ions are left behind, forming the channel boundary.

In time, the forward propagating front exhibits dispersive behaviour. An electric field develops across the main front due to charge separation. The electric field is zero at the peak of the front, developing a positive field ahead of the density perturbation and a negative field to its rear, respectively. Electrons and ions start to lag the main front and form the emergent backfill of the previously formed cavity.

Over the duration of the simulation the electric field across the front reduces in accordance with energy dissipation and the loss of electrons and ions to the quasi-neutral, forward propagating front, and the quasi-neutral plasma that lags the principal front. This is demonstrated more clearly in figure 7 where the electric field, E_2 , and electron density are plotted on the same axis scales. These observations are in qualitative agreement with the previous work of Krushelnick *et al* [2] and Sarkisov *et al* [5] at lower intensities.

5. DISCUSSION

In this Report, optical probing measurements have been presented of the underdense helium plasma response following the passage of a sub-ps laser pulse at intensities of greater than $10^{20} \text{ W cm}^{-2}$. Interesting features include the reduction in front thickness in time and the onset of instabilities without

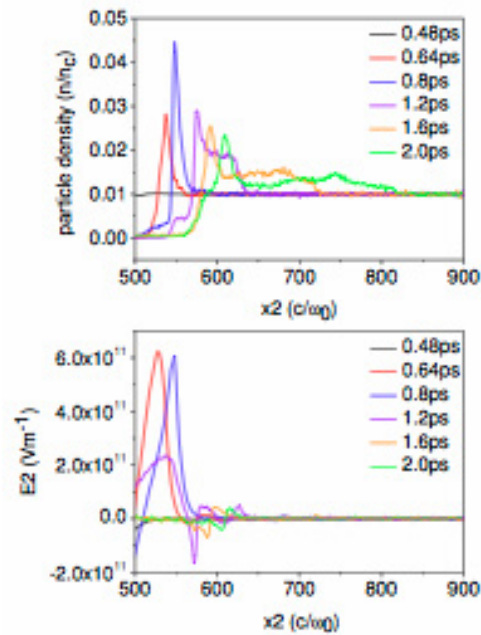


Figure 7. OSIRIS code results for different time steps showing the evolution of electron density (left) and the magnitude of the radial electric field (right).

the front breaking-up or fragmenting. This is different to the case of a hydrodynamic front that increases in thickness as it snow ploughs into the ambient medium, expected to form on longer timescales than are discussed here. The underlying cause of this behaviour is currently under study, likely to be caused by the affect of relativistic self-focusing on energy-coupling to hot electrons and the resulting multi-group flux of ions generated by the Coulomb explosion mechanism, highlighted by the OSIRIS simulations.

The environment and shock front created here are very different to those recently reported at lower intensities and presents the opportunity to study different classes of blast front and their associated instabilities. Not least, this creates an environment in which to study the transition from weakly collisional to collision dominated behaviour, prior to the classic Sedov-Taylor limit.

References

- [1] A Modena et al, *Nature*, 377, 606 (1995).
- [2] K Krushelnick et al, *PRL* 83, 4 (1999); R A Snavely et al, *PRL* 85, 2945 (2000).
- [3] M Dunne et al, *PRL* 72, 7 (1994); T Clark and H Milchberg, *PRL* 78, 12 (1997); J Gruun et al *PRL* 66, 2738 (1991); T Ditmire et al *PRL* 80, 4 (1998); M J Edwards et al, *PRL* 87, 8 (2001).
- [4] R Chevalier, *Ann. Rev. Astron. Astrophys.* 15, 175 (1977), E T Vishniac, *ApJ* 428, 186 (1994); E T Vishniac, *ApJ* 274, 152 (1983).
- [5] G S Sarkisov et al, *PRE* 59, 6 (1999).